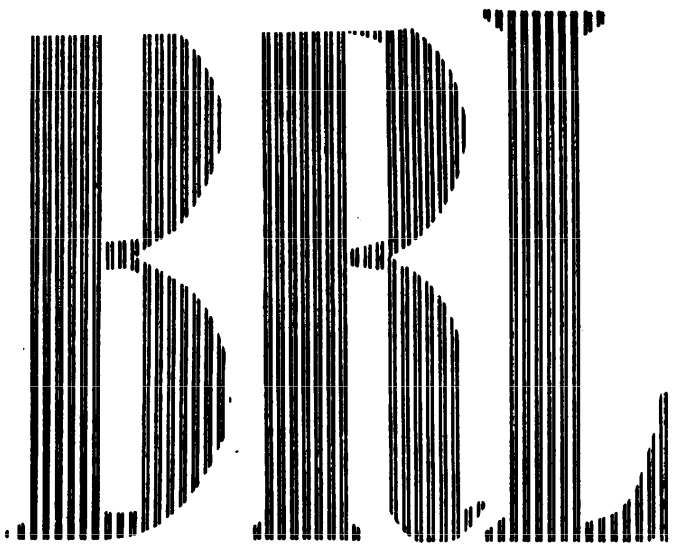

REPORT NO. 1099
March 1960

SOME ASPECTS OF NON-EQUILIBRIUM FLOWS

Raymond Sedney

Department of the Army Project No. 5B03-03-001
Ordnance Management Structure Code No. 5010.11.814
BALLISTIC RESEARCH LABORATORIES

ABERDEEN PROVING GROUND, MARYLAND

Destroy when no longer needed. DO NOT RETURN

B A L L I S T I C R E S E A R C H L A B O R A T O R I E S

REPORT NO. 1099

MARCH 1960

SOME ASPECTS OF NON-EQUILIBRIUM FLOWS

Raymond Sedney

Department of the Army Project No. 5B03-03-001
Ordnance Management Structure Code 5010.11.814
(Ordnance Research and Development Project No. TB3-0108)

A B E R D E E N P R O V I N G G R O U N D, M A R Y L A N D

B A L L I S T I C R E S E A R C H L A B O R A T O R I E S

REPORT NO. 1099

RSedney/sec
Aberdeen Proving Ground, Md.
March 1960

SOME ASPECTS OF NON-EQUILIBRIUM FLOWS

SUMMARY

In this paper some of the general features of non-equilibrium flow are discussed. In particular, vibrational relaxation is discussed in detail. This case is somewhat simpler than dissociation and ionization but it illustrates some of the main new features of non-equilibrium flow. Those aspects of two-dimensional and axisymmetric flow behind shock waves are examined analytically which yield significant information without requiring numerical solution of the governing equations.

The thermodynamics of a vibrational relaxing gas is discussed. The conditions for simulating flows are noted. Crocco's theorem and the characteristic equations are derived. Then a simple method of obtaining the initial gradients of the flow variables behind a shock is shown. These gradients are used in discussing two particular flows. An exact solution for flow over a cusped body is obtained. Flow over a wedge near the tip and far from the tip is considered. It is found that far from the tip a boundary layer type phenomenon occurs.

NOTATION

C_p		pressure coefficient
c_p, c_v		specific heats at constant pressure, volume respectively
D	=	$1 - M_a^2 + \cot^2 \lambda$
$D_{\pm}$		operator for differentiation along characteristics
E_i		internal energy
e_i	=	$\left[E_i (T_a) - E_i (T_\infty)\right] / RT_a$
$F_{1,2,3,4}$		coefficients in gradient functions
f_1		$\left[E_i (T_a) - E_i (T_\infty)\right] / (c_{p_a} T_a \tau q)$
f_2	=	$T_a \partial S/\partial \beta$
h		enthalpy
K_w		curvature of shock wave
K_s		curvature of streamline
ℓ		displacement of shock, Figure 7(c)
M		Mach number
n		coordinate along normal to streamline
p		pressure
q		velocity
R		gas constant (per molecular weight of gas)
r		radial polar coordinate
S		entropy
s		coordinate along streamline
T		temperature
t		time
x		coordinate in free stream direction
y		coordinate normal to free stream direction
α	=	$\theta - \phi$
β		shock wave angle
γ		ratio of specific heats
ϵ	=	0 or 1 for two-dimensional or axisymmetric flow respectively

ζ		vorticity
η		coordinate along shock wave
θ		direction of velocity vector
θ_v		characteristic vibrational temperature
λ	=	$\beta - \theta$, behind shock wave
μ	=	$\sin^{-1}(1/M_a)$
ξ		coordinate normal to shock wave
ξ_r		relaxation distance (equation 5.12)
ρ		density
σ		distance along shock
τ		relaxation time
ϕ		angular polar coordinate
Ψ	=	$\beta - \theta$
ω		vorticity

Subscripts:

a	active degrees of freedom (translation and rotation)
i	internal degree of freedom (vibration)
e	equilibrium conditions
f	frozen conditions
t	stagnation conditions
∞	free stream conditions

1. INTRODUCTION

There have been many recent publications considering the flow of a gas not in thermodynamic equilibrium. No complete bibliography will be given here, but several papers pertinent to the present work will be mentioned.

Probably the first work on this subject, for the case where there are shock waves in the flow, is that of Bethe and Teller[1]. A qualitative discussion of flow over a wedge was given by Ivey and Cline[2] in which the departure from thermodynamic equilibrium was due to vibrational relaxation of a diatomic gas. (Some quantitative results will be given here for this case.) An approximation to the hypersonic flow over a sphere, where the departure from equilibrium is due to dissociation, was considered by Freeman[3]. Flows with small disturbances were considered by Moore and Gibson[4], and in particular, the flow over a thin wedge.

In a pure diatomic gas at reasonable temperatures, three processes can cause departure from equilibrium: vibrational excitation, dissociation, and ionization. If the relaxation times for these processes are sufficiently different, they may be treated separately. The magnitude of the effects on the flow variables due to the three processes is quite different. The gross effects are directly related to the energy necessary to excite the new degrees of freedom.

In this paper vibrational relaxation only is considered. This is somewhat simpler to handle than dissociation and ionization, but should illustrate some of the main features of non-equilibrium flow. Because the smallest non-equilibrium effects result from vibrational excitation, some of the results obtained here differ little from the results of calculations based on equilibrium flow; or differences are significant only in a negligibly small region of flow. It is hoped that the methods used here can be applied, with almost equal ease, to other non-equilibrium processes.

Only certain aspects of two-dimensional and axisymmetric flows are examined in this paper; these will not involve numerical solution of the differential equations. After a discussion of the appropriate thermodynamics of a vibrational relaxing diatomic gas, the governing equations are transformed to yield the generalization of Crocco's theorem which relates the entropy change to the vorticity. Next a derivation and discussion of the characteristic equations are given. Using the appropriate shock transition relations and the equations of motion, the streamwise gradients of the flow variables are obtained employing natural coordinates (as indicated by Sternberg[5] for equilibrium flows.) These prove to be quite useful in discussing two particular flows; namely, two dimensional flow over (i) a cusped body which supports a straight shock wave, and (ii) a wedge.

For (i) an exact solution is obtained that requires only two quadratures. For (ii) the flow is examined near the tip and far from the tip. At the tip the shock curvature and the wedge pressure gradient can be obtained rather simply using the gradient functions. Far from the tip the flow must be divided into two regions. To a first approximation a large region of the flow is the equilibrium wedge flow, but there is a small region near the shock wave where relaxation is important. Mathematically this small region exhibits a boundary layer type phenomenon. An indication is given of a means of obtaining the next approximation.

2. THERMODYNAMICS

Basically the difference in the descriptions of equilibrium and non-equilibrium flows results from differences in the thermodynamic behavior of the gas, the dynamic aspects being the same. A clear explanation of an appropriate model of a non-equilibrium system (and the necessary assumptions) was given by Wood and Kirkwood[6]. The same model will be used here.

For the case of a gas subject to vibrational relaxation the degrees of freedom are divided into two classes: the active (translation and rotation), for which the subscript a will be used, and the internal or inert (vibration), for which the subscript i will be used. It is assumed that local thermodynamic equilibrium exists within the classes but not between them. The rate at which equilibrium is approached is governed by a rate equation which can be specified in terms of the state variables of each class. There are other assumptions, to be mentioned later, which are convenient to make. The model presented[6] is intermediate between a macroscopic and a microscopic description.

From the assumption that the Gibbs relation holds for the "a" class, it follows that the entropy change of the "a" class is

$$dS_a = c_{p_a}\, dT_a/T_a - R\, dp/p,$$

where the perfect gas law is assumed

$$p = \rho\, R\, T_a \tag{2.1}$$

It is assumed that the "i" class is specified by its temperature, T_i, so that the entropy change is

$$dS_i = dE_i/T_i$$

The total entropy change is then

$$dS = dS_a + dS_i$$

$$= c_{p_a}\, d\, T_a/T_a - R\, dp/p + dE_i/T_i \tag{2.2}$$

The rate equation assumed is the linear form

$$dE_i/dt = \left[E_i(T_a) - E_i\right] \quad /\tau \tag{2.3}$$

where τ is the relaxation time and $E_i\ (T_a)$ is the value of E_i if equilibrium existed at the temperature T_a. For a flow the derivative in (2.3) is the substantial derivative.

The linear form of the rate equation presupposes that the departure from equilibrium is not too great. It is exact if the vibrators are quantized harmonic oscillators.[1] The functional relation $E_i(T_a)$, for various gases, can be obtained from tables of the properties of gases.[7] With the assumption of harmonic oscillators, $E_i(T_a)$ can be calculated from

$$E_i\ (T_a) = R\ \Theta_v/ \quad \left[\exp.\ (\Theta_v/T_a) - 1\right] \quad ; \tag{2.4}$$

where Θ_v is the characteristic vibrational temperature. This form will be used when some specific flows are calculated. It is convenient, though not necessary, to carry along both variables E_i and T_i. The functional dependence $E_i(T_i)$, for the case of harmonic oscillators, has the same form as $E_i(T_a)$ in (2.4).

For future reference the following well known relations are recorded. For equilibrium flow $T_a = T_i$ and

$$c_p - c_v = R$$

where

$$c_p = c_{p_a} + c_i$$

$$c_v = c_{v_a} + c_i$$

$$c_i = d\ E_i/dT_a.$$

Also

$$c_{p_a} - c_{v_a} = R.$$

3. EQUATIONS OF MOTION

In this section the equations of motion of a pure diatomic gas subject to vibrational relaxation will be discussed. The equation of state (2.1) is assumed. By a minor modification the results can be extended to the case of a mixture of diatomic gases where only one constituent relaxes. It is necessary to know the effect of the other constituents on this one. This case would arise, in practice, if the relaxation time of one constituent is much shorter than that of the others. This would be the case for air since the relaxation time of oxygen is about one-fifteenth that of nitrogen. This extension, however, will not be included here.

The equations will be written in natural coordinates (s, n), where s and n are distances along the streamlines and their orthogonal trajectories, respectively. The form of the equations of conservation of momentum, mass, and energy do not change because of relaxation; they are

$$\rho\, q\, \partial q/\partial s = -\, \partial p/\partial s \tag{3.1}$$

$$\rho\, q^2\, \partial\theta/\partial s = -\, \partial p/\partial n \tag{3.2}$$

$$\frac{1}{\rho}\,\frac{\partial \rho}{\partial s} + \frac{1}{q}\,\frac{\partial q}{\partial s} + \frac{\partial \theta}{\partial n} + \frac{\epsilon \sin\theta}{y} = 0 \tag{3.3}$$

$$h + (q^2/2) = h_t \tag{3.4}$$

where q is velocity, θ is the velocity direction, $\epsilon = 0$ or 1 for two-dimensional or axisymmetric flow, respectively; y is the coordinate perpendicular to the axis of symmetry; $h = c_{v_a} T_a + E_i + p/\rho$ is the enthalpy; and h_t is the stagnation enthalpy (constant along streamlines). These four equations, together with the equation of state (2.1) and the rate equation, give a complete description of the flow. In natural coordinates the rate equation (2.3) is

$$q\, \partial E_i/\partial s = \left[E_i(T_a) - E_i\right] \Big/ \tau \tag{3.5}$$

The relaxation time, τ, is a function of pressure and temperature. In the following it is assumed to be constant. This would be a poor assumption if there are large changes in pressure and temperature; however, in the regions of flow considered changes of appreciable magnitude in these quantities do not occur.

For the above six equations, the conditions for similar flows over geometrically similar bodies are easily deduced. In addition to the requirements of fixed Mach number and ratio of specific heats, $\tau\, U/\ell$ must also be fixed for similar flows. Here U and ℓ are representative velocity and length, respectively. This type of dimensionless ratio was used by Freeman[3]. Experimentally the appearance of the new length scale τU makes simulation more difficult. Analytically it means that the simple "similarity solutions" (wedge flow and Prandtl-Meyer expansion) no longer exist.

A useful relation for equilibrium flows is Crocco's theorem.[9] It relates the entropy gradient to the vorticity. For a relaxing gas this relation can be derived as follows. The expression for the entropy change (2.2) can also be written

$$T_a\, dS = dh - dp/\rho - \left[1 - (T_a/T_i)\right] \quad d\, E_i$$

Using (3.4) to eliminate h,

$$T_a\, dS = dh_t - q\, dq - dp/\rho - \left[1 - (T_a/T_i)\right] \quad d\, E_i$$

From this the directional derivatives of S in the s and n directions are evaluated. After elimination of the pressure by use of the momentun equations (3.1) and (3.2), these derivatives are expressible as

$$T_a\, \partial S/\partial s = - \left[1 - (T_a/T_i)\right] \quad \partial E_i/\partial s \qquad (3.6)$$

$$T_a\, \partial S/\partial n = q\zeta - \left[1 - (T_a/T_i)\right] \quad \partial E_i/\partial n + dh_t/dn \qquad (3.7)$$

where ζ is the vorticity,

$$\zeta = q\, \partial\theta/\partial s - \partial q/\partial n$$

Note that $\partial h_t/\partial s = 0$, but $\partial h_t/\partial n = 0$ only for isoenergetic flows. If the flow is in equilibrium, $T_a = T_i$, (3.6) gives the result of constant entropy along streamlines, and (3.7) reduces to the usual form of Crocco's theorem. For three-dimensional unsteady flow the vector form of Crocco's theorem is

$$\partial\vec{q}/\partial t - \vec{q} \times \vec{\omega} = T_a \overset{\uparrow}{\nabla} S - \overset{\uparrow}{\nabla} h_t + \left[1 - (T_a/T_i)\right] \overset{\uparrow}{\nabla} E_i$$

where $\vec{\omega}$ is the vorticity vector and $\overset{\uparrow}{\nabla}$ is the gradient operator. An equivalent result, but in different thermodynamic variables, was given by Broer.[10]

It is convenient to eliminate p and ρ from the equations of motion and introduce S. The resulting equations for isoenergetic flow are

$$(M_a^2 - 1)\frac{\partial q}{\partial s} - q\frac{\partial \theta}{\partial n} = \frac{\epsilon\, q \sin\theta}{y} + \left(\frac{q}{c_{p_a} T_a}\right)\frac{\partial E_i}{\partial s} \qquad (3.8)$$

$$q^2\, \partial\theta/\partial s - q\, \partial q/\partial n = T_a\, \partial S/\partial n + \left[1 - (T_a/T_i)\right]\, \partial E_i/\partial n \qquad (3.9)$$

$$T_a\, \partial S/\partial s + \left[1 - (T_a/T_i)\right]\, \partial E_i/\partial s = 0 \qquad (3.10)$$

$$q\, \partial E_i/\partial s = \left[E_i(T_a) - E_i\right]/\tau \qquad (3.11)$$

$$c_{p_a} T_a + E_i + (q^2/2) = h_t \qquad (3.12)$$

where

$$M_a^2 = q^2\, c_{v_a}/(c_{p_a} R\, T_a).$$

Thus only the "frozen" Mach number enters. Note that (3.9) and (3.10) are simply (3.6) and (3.7) while (3.8) comes from (2.1), (3.1), (3.3), and the expression for $\partial S/\partial s$. The unknowns are q, θ, T_a, E_i, and S.

It is easily verified by the standard technique that the above partial differential equations are hyperbolic if $M_a > 1$. Solving the determinant equation for the four characteristic directions, one obtains the streamline

direction counted twice and the Mach lines based on M_a; that is, the Mach angle is $\mu = \sin^{-1}(1/M_a)$. The equations of motion in characteristic form are (3.10), (3.11), and the following two equations:

$$\cot \mu \, D_{\pm} q \mp q \, D_{\pm} \theta = \frac{\epsilon \, q \sin \theta \sin \mu}{y} + \frac{\sin \mu \left[E_i(T_a) - E_i \right]}{\tau \, c_{p_a} \, T_a}$$

$$- \cot \mu \left\{ T_a \, D_{\pm} S + \left[1 - (T_a/T_i) \right] \, D_{\pm} E_i \right\} / q \qquad (3.13)$$

where the operators $D_{\pm}$ are defined by

$$\sec \mu \, D_{\pm} = \partial/\partial s \pm \tan \mu \, \partial/\partial n;$$

that is, $D_{\pm}$ indicates differentiation along the Mach lines inclined at $\pm \mu$ to the streamline. The appearance of the "frozen" Mach lines has been noted by other authors.[6,10] A numerical calculation, using the characteristic form, for flow over a wedge is in progress and will be reported in another paper.

4. GRADIENTS BEHIND A SHOCK WAVE

A general method for computing the flow variable gradients behind a shock wave in a two-dimensional flow was developed by Thomas[11] for a gas not subject to relaxation effects. A simpler method, using natural coordinates, was indicated by Sternberg.[5] For two-dimensional flow the gradients are particularly useful; e.g., the slope of the streamlines at shock polar points in the hodograph plane can be obtained from them (the so-called "hedge-hog" introduced by Busemann). It is found that the gradients are proportional to the shock wave curvature.

For axisymmetric flow the same gradients can be computed, but they are linear combinations of the two curvatures: K_w in the meridianal and $1/y$ in the azimuthal planes. This fact limits the usefulness of the gradients for this case. Extensive tabulations have been made recently[12] of the coefficients of K_w and $1/y$; with these the gradients can be computed easily. (The two-dimensional result is obtained by setting the coefficient of $1/y$ equal to zero.)

For a uniform flow which is in equilibrium in front of a shock wave but not behind it, the gradients will depend on the relaxation time. Behind the shock the flow variables are computed from the shock relations for constant specific heats; i.e., the frozen relations.[9] E_i does not change across a shock.[1] To obtain expressions for the gradients, the equations of motion are combined with the shock relations; the normal derivatives are expressed in terms of derivatives along the shock wave and along the streamline. Referring to Figure 1,

$$\partial/\partial\sigma = \cos\lambda\ \partial/\partial s + \sin\lambda\ \partial/\partial n$$

where σ is distance along the shock wave, β is the shock angle, and $\lambda = \beta - \theta$. Since

$$\partial/\partial\sigma = \partial\beta/\partial\sigma\ (\partial/\partial\beta) = K_w\ \partial/\partial\beta$$

the normal derivative can be written

$$\partial/\partial n = \left[K_w\ \partial/\partial\beta - \cos\lambda\ \partial/\partial s\right] \Big/ \sin\lambda \qquad (4.1)$$

The normal derivatives in (3.8) and (3.9) are eliminated by use of (4.1); $\partial E_i/\partial\beta = 0$, and $\partial q/\partial\beta$, $\partial\theta/\partial\beta$, etc. can be computed from the shock relations. The following two equations then result:

$$(M_a^2 - 1)\,\partial q/q\partial s + \cot\lambda\,\partial\theta/\partial s = (\epsilon/y)\sin\theta + f_1 + (K_w k_2/\sin\lambda) \tag{4.2}$$

$$\cot\lambda\,\partial q/\partial s + q\,\partial\theta/\partial s = K_w\,(f_2 + g\,k_1)/(q\sin\lambda) \tag{4.3}$$

where

$$k_1 = \partial q/\partial\beta, \qquad k_2 = \partial\theta/\partial\beta$$

$$f_1 = (\partial E_i/\partial s)/c_{p_a} T_a = \left[E_i\,(T_a) - E_i\,(T_\infty)\right]/(c_{p_a} T_a\,\tau\,q)$$

$$f_2 = T_a\,\partial S/\partial\beta$$

and all quantities are evaluated immediately behind the shock wave. Solving (4.2) and (4.3) for $\partial\theta/\partial s$ and $\partial q/\partial s$, one obtains

$$\partial\theta/\partial s = F_1 K_w + (\epsilon/y)\,F_2 + (f_1\cot\lambda)/D \tag{4.4}$$

$$(1/q_\infty)\,\partial q/\partial s = F_3 K_w + (\epsilon/y)\,F_4 - q\,f_1/(q_\infty D) \tag{4.5}$$

where

$$F_1 = \left[(1 - M_a^2)(k_1 + f_2\,q^{-1}) + q\,k_2\cot\lambda\right]\;/\;(q\,D\sin\lambda)$$

$$F_2 = (\sin\theta\cot\lambda)/D$$

$$F_3 = \left[(k_1 + f_2\,q^{-1})\cot\lambda - q\,k_2\right]\;/(q_\infty\,D\sin\lambda)$$

$$F_4 = -(q\sin\theta)/(q_\infty\,D)$$

$$D = 1 - M_a^2 + \cot^2\lambda$$

The F_i are functions of M_∞, β, and γ, and have been tabulated[12] for $\gamma = 1.4$, $1.1 \leq M_\infty \leq 10$, and $\sin^{-1}(1/M_\infty) < \beta \leq \pi/2$.

By use of (3.1), (3.3), and (3.4) the gradients of p, ρ, and T_a can be obtained, Since f_1 and D are positive, the effect of relaxation is to increase the streamline curvature $\partial\theta/\partial s$ and decrease the velocity gradient for given K_w and y. For reasonably strong shocks at ordinary T_∞, $E_i\ (T_\infty)$ can be neglected compared to $E_i\ (T_a)$.

Even for two dimensional flows it is seen that the gradients will not be simply proportional to K_w; this will limit their usefulness. Some application will be made of these gradients in the next two chapters.

5. AN EXACT SOLUTION

As mentioned previously, the solution for flow over a wedge is no longer simple when the gas behind the shock is relaxing; the flow behind the shock is not uniform and the shock is not straight. This flow will be considered in the next section. Here it will be shown that an exact solution can be obtained for two-dimensional flow over a cusped body (the curvature becoming zero asymptotically) which supports a straight shock wave.

From (4.4), with $\epsilon = 0$, it can be seen that if the shock is locally straight, $K_w = 0$, the curvature of the streamline at the shock can be easily calculated. Letting $K_s = \partial\theta/\partial s$, a convenient non-dimensional measure of streamline curvature is the following quantity:

$$K_s \tau q_\infty / e_i = (R q_\infty \cot \lambda)/c_{p_a} q D \qquad (5.1)$$

where

$$e_i = \left[E_i (T_a) - E_i (T_\infty)\right] / RT_a \qquad (5.2)$$

A plot of the expression in (5.1) is shown in Figure 2 for a range of values of M_∞ and β. For the case of pure N_2 with $T_\infty = 300^\circ K$, $\beta = 60^\circ$, $M_\infty = 6$, where (2.4) was used with $\theta_v = 3336^\circ K$, it is found that $\theta = 41.1$ and $K_s = 5.5$ ft^{-1}. The value of τ was taken from Reference 8.

Since (5.1) has no physical length scale in it, the shock wave could be straight over any finite distance and K_s would be the same everywhere. Considering the manner in which a numerical solution of the characteristic equations would proceed, starting from a straight shock, one can see that all the flow variables depend only on the distance along the normal to the shock. A "shock oriented" coordinate system ξ, η is introduced, as shown in Figure 3, and a solution with flow variables independent of η is sought. The streamlines will be parallel curves with initial curvature given by K_s in (5.1) and initial slope calculated from the frozen shock relations. If the streamlines are physically meaningful, any one of them can be chosen as the body. Reflecting this curve through the free stream

direction gives a pointed cusped body which supports a straight shock wave. Anticipating a result from the next chapter, the curvature of the body should approach zero and the angle of the body should approach the equilibrium wedge angle appropriate to the given shock angle. These expectations are verified by the solution obtained below.

Equations (3.8) to (3.12) are transformed to the (ξ, η) system by

$$\partial/\partial s = \sin(\beta - \theta)\, \partial/\partial\xi + \cos(\beta - \theta)\, \partial/\partial\eta$$

$$\partial/\partial n = -\cos(\beta - \theta)\, \partial/\partial\xi + \sin(\beta - \theta)\, \partial/\partial\eta$$

Setting all η derivatives equal to zero and letting

$$\psi = \beta - \theta,$$

one obtains the following equations:

$$(M_a^2 - 1) \sin\psi \frac{\partial q}{\partial \xi} + q \cos\psi \frac{\partial \theta}{\partial \xi} = \frac{q \sin\psi}{c_{p_a} T_a} \frac{\partial E_i}{\partial \xi} \tag{5.3}$$

$$q \sin\psi\, \partial\theta/\partial\xi + \cos\psi\, \partial q/\partial\xi = 0 \tag{5.4}$$

$$T_a\, \partial S/\partial\xi + \left[1 - (T_a/T_i)\right] \partial E_i/\partial\xi = 0 \tag{5.5}$$

$$q \sin\psi\, \partial E_i/\partial\xi = \left[E_i(T_a) - E_i\right]/\tau \tag{5.6}$$

$$c_{p_a} T_a + E_i + (q^2/2) = h_t \tag{5.7}$$

On elimination of ξ, (5.4) can be written

$$dq/q = -\tan\psi\, d\theta$$

Integrating,

$$q \cos\psi = q_f \cos(\beta - \theta_f), \tag{5.8}$$

where the subscript f denotes values computed from the frozen shock relations.

Combining (5.3) with the differentiated form of (5.7) and eliminating ξ, a first order ordinary differential equation is obtained. The result of integrating this is

$$T_a = \left[T_{a_f} + (q_f^2/R) \sin^2 (\beta - \theta_f)\right] \cot (\beta - \theta_f) \tan \psi - (q_f^2/R) \cos^2 (\beta - \theta_f) \tan^2 \psi \tag{5.9}$$

where again the frozen shock relations have been applied. E_i is obtained from (5.7), with the aid of (5.8) and (5.9).

$$E_i = h_t + \left[(c_{p_a}/R)\tan^2 \psi - (1/2) \sec^2 \psi\right] q_f^2 \cos^2 (\beta - \theta_f) - c_{p_a}\left[T_{a_f} + (q_f^2/R) \sin^2 (\beta - \theta_f)\right] \cot (\beta - \theta_f) \tan \psi \tag{5.10}$$

With all the variables expressed in terms of θ, (5.6) can now be used to obtain θ as a function of ξ. Thus

$$\xi = q_f \tau \cos (\beta - \theta_f) \int_{\theta_f}^{\theta} F(\theta)\, d\theta$$

$$F(\theta) = \tan \psi \, (dE_i/d\theta) / \left[(E_i (T_a) - E_i\right]$$

The equation of the body is, in parametric form (parameter θ_b),

$$\xi_b = q_f \tau \cos (\beta - \theta_f) \int_{\theta_f}^{\theta_b} F(\theta)\, d\theta$$

$$\eta_b = q_f \tau \cos (\beta - \theta_f) \int_{\theta_f}^{\theta_b} \left[F(\theta)/\tan \psi\right] d\theta$$

The above integrations are carried out until $E_i(T_a)$ is equal to E_i; that is, equilibrium is attained. In principle, ξ_b and η_b become infinite for

this condition; actually, the curvature of the body approaches zero rather quickly and the gas is, for all practical purposes, in equilibrium at finite ξ_b and η_b.

A representative result (obtained by numerical integration) of the above formulas is shown in Figure 4 for N_2 at $M_\infty = 8$, $\beta = 65^\circ$, $T_\infty = 300^\circ K$. Equations (2.4) was used to obtain $E_i(T_a)$, with $\theta_v = 3336^\circ K$. The angle of the body changes about three degrees from $\theta_f = 43.6^\circ$ to $\theta_e = 46.7^\circ$, the latter being the wedge angle that corresponds to a shock angle of 65° when the equilibrium shock relations are used. For the latter relations see, e.g., Reference 13. The largest change in angle occurs when θ_f and M_∞ are close to the conditions for shock detachment in frozen flow.

Thus an exact calculation (with two quadratures) of the flow with a straight shock wave is possible. These results can be used to check approximate methods of computing flows. In the next chapter this exact solution will be used to investigate a portion of the flow far from the tip of a wedge.

It is desirable to define some measure of the distance over which relaxation effects are important. As in defining the thickness of a viscous boundary layer, there is some arbitrariness in any definition of a relaxation distance. Following Moore and Gibson[4], one such definition would be

$$\int_0^\infty \left[1 - (E_i/E_{i_{eq.}})\right] \, d\xi,$$

where $E_{i_{eq.}}$ is the final equilibrium value of E_i. If $E_{i_{eq.}}$ is replaced by $E_i(T_a)$, the value of the integral would not be changed much, but the integration would be easier. Calling this relaxation distance ξ_r,

$$\xi_r = \int_o^\infty \left[1 - E_i/E_i(T_a) \right] \, d\xi$$

$$= q_f \tau \cos(\beta - \theta_f) \int_{\theta_f}^{\theta_e} \left[(dE_i/d\theta) \tan \psi / E_i(T_a) \, d\theta \right] \qquad (5.12)$$

where θ_e is the equilibrium wedge angle. For the particular example cited above

$$\xi_r = .136 \, q_\infty \, \tau = .300 \, q_f \, \tau$$

No reason was given for the particular definition of a relaxation distance in Reference 4; it is analogous to the definition of displacement thickness of a viscous boundary layer. In the next chapter a different method of obtaining a distance is given which results in a coefficient of $\tau \, q_\infty$ thirty per cent higher than the one given for ξ_r.

6. FLOW OVER A WEDGE

Several years ago Ivey and Cline[2] discussed the two-dimensional flow over a wedge. This was mainly a qualitative discussion. However, it was pointed out that at the tip the shock wave should have the angle appropriate to the frozen shock relations, and far from the tip the (smaller) angle appropriate to the equilibrium shock relations[13]. Also the shock curve is concave downward. Here some further quantitative results for this flow are shown.

It seems most natural to use polar coordinates (r, ϕ) with the origin at the tip and ϕ measured from the free stream direction. Transforming Equations (3.8) to (3.12), with $\epsilon = 0$, to polar coordinates gives

$$(M_a^2 - 1)(r \cos \alpha \, \partial q/\partial r + \sin \alpha \, \partial q/\partial \phi) + q(r \sin \alpha \, \partial \theta/\partial r - \cos \alpha \, \partial \theta/\partial \phi)$$
$$= (q/c_{p_a} T_a)(r \cos \alpha \, \partial E_i/\partial r + \sin \alpha \, \partial E_i/\partial \phi) \tag{6.1}$$

$$q^2(r \cos \alpha \, \partial \theta/\partial r + \sin \alpha \, \partial \theta/\partial \phi) + q(r \sin \alpha \, \partial q/\partial r - \cos \alpha \, \partial q/\partial \phi)$$
$$= - T_a (r \sin \alpha \, \partial S/\partial r - \cos \alpha \, \partial S/\partial \phi) \tag{6.2}$$
$$- \left[1 - (T_a/T_i)\right] (r \sin \alpha \, \partial E_i/\partial r - \cos \alpha \, \partial S/\partial \phi)$$

$$T_a (r \cos \alpha \, \partial S/\partial r + \sin \alpha \, \partial S/\partial \phi) =$$
$$- \left[1 - (T_a/T_i)\right] (r \cos \alpha \, \partial E_i/\partial r + \sin \alpha \, \partial E_i/\partial \phi) \tag{6.3}$$

$$q(r \cos \alpha \, \partial E_i/\partial r + \sin \alpha \, \partial E_i/\partial \phi) = (r/\tau) \left[E_i(T_a) - E_i\right] \tag{6.4}$$

$$c_{p_a} T_a + E_i + (q^2/2) = h_t \tag{6.5}$$

where $\alpha = \theta - \phi$

To consider the flow near the tip a dimensionless variable, $r/\tau q_\infty$, is introduced. Until the appropriate boundary conditions for wedge flow are introduced, the following discussion applies to any two-dimensional

flow (e.g., the modifications to Prandtl-Meyer flow over a corner). Assume that all the flow variables can be expanded in a power series in $r/\tau q_{\infty}$; then it can be shown that, to within $O(r/\tau q_{\infty})$ terms, the flow is frozen. The form of these series would be

$$f(r,\phi) = f_o(\phi) + (r/\tau q_{\infty})\, f_1(\phi) + \ldots\ldots$$

The zeroth order terms satisfy

$$(M_{a_o}^{\ 2} - 1) \sin \alpha_o \, \partial q_o/\partial\phi - q_o \cos \alpha_o \, \partial\theta_o/\partial\phi = 0 \qquad (6.6)$$

$$\cos \alpha_o \, \partial q_o/\partial\phi - q_o \sin \alpha_o \, \partial\theta_o/\partial\phi = 0 \qquad (6.7)$$

$$\partial S_o/\partial\phi = 0 \qquad (6.8)$$

$$\partial E_{i_o}/\partial\phi = 0 \qquad (6.9)$$

Equations (6.6) and (6.7) present two possibilities; either

$$M_{a_o}^{\ 2} \sin^2 \alpha_o = 1,$$

which is appropriate for corner flow, or

$$\partial q_o/\partial\phi = \partial\theta_o/\partial\phi = 0,$$

which, after applying the wedge boundary conditions, gives frozen flow over a wedge. To within an error $O(r/\tau q_{\infty})$, the shock wave is straight.

The next step would be the solution of the differential equations for q_1, θ_1, etc. Although this is feasible, it will not be done because the most interesting information can be more easily obtained from the gradient functions of Chapter 4. Since, for the wedge, $\partial\theta/\partial s = 0$, the curvature of the shock at the tip is, from (4.4),

$$K_w = - (f_1 \cot \lambda)/DF_1$$

The frozen values of the variables are used in the right hand side. In non-dimensional form

$$K_w \tau q_\infty / e_i = - (R q_\infty \cot \lambda)/c_{p_a} q \, DF_1 \qquad (6.10)$$

A plot of the expression in (6.10) is shown in Figure 5 for a range of M_∞ and β. For the case of pure N_2 with $T_\infty = 300^\circ K$, $\beta = 60^\circ$, $M_\infty = 6$, $p_\infty = 1$ atm.,

$$\theta = 41.1^\circ, \quad K_w = 4.1 \text{ ft}^{-1}$$

where (2.4) was used with $\theta_v = 3336^\circ$ K; the value of τ was taken from Reference 8, and F_1 from Reference 12. For the same conditions, except $M_\infty = 10$, K_w is 220 ft^{-1}, which means that the curvature would not be detectable in any ordinary scale of experiment.

With K_w known, the initial velocity gradient along the wedge can be computed from (4.5), and then the pressure gradient from (3.1). A convenient non-dimensional form for the pressure coefficient is

$$(\partial C_p/\partial s)(\tau q_\infty / e_i) = 2(\rho q/\rho_\infty q_\infty) \left[(R/c_{p_a} D) - (F_3 K_w \tau q_\infty / e_i) \right] \qquad (6.11)$$

where

$$C_p = 2(p - p_\infty)/\rho_\infty q_\infty^{\,2}$$

A plot of the expression in (6.11) is shown in Figure 6. For the above example ($M_\infty = 6$) $\partial C_p/\partial s = 16.0$ ft.^{-1}

Thus the shock curvature and the rate of change of the flow variables on the wedge at its tip can be obtained rather easily; if the details of the flow are desired, the series expansion method should be used. Unfortunately, the same method, i.e. employing the gradient functions, cannot be used to investigate cone flow. The use of natural coordinates at the tip of a cone is impossible because of the nature of the singularity there. The series expansion method could be used, but the differential equations for the first order terms would be much more difficult to solve than those of the wedge case.

To consider the flow far from the tip, a series expansion procedure is again adopted, but now $\tau q_\infty / r$ is the variable. The assumption that the flow variables are analytic in this variable will be seen to be not uniformly valid. The difference between this case and the previous one can be seen by examining (6.4). When $r/\tau q_\infty$ approaches zero, the right hand side vanishes and nothing unusual happens. When $\tau q_\infty / r$ approaches zero, the left hand side vanishes and the result is that $E_i\ (T_a) = E_i$; that is, the flow is in equilibrium. Since derivatives have been lost, a boundary layer type phenomenon (singular perturbation) must be expected. The order of the system (6.1) to (6.4) is reduced from four to three by this limiting process. Also the result that the flow is in equilibrium is inconsistent with the boundary condition $E_i = E_{i_\infty}$ at the shock.

If the flow variables are expanded in a series of the form

$$f(r, \phi) = f^{(o)}\ (\phi) + (\tau\ q_\infty / r)\ f^{(1)}\ (\phi) + \ldots .$$

the zeroth order terms for q and θ will satisfy equations of the same form as (6.6) and (6.7) except with zero superscripts instead of subscripts and M_a replaced by the equilibrium Mach number. Thus, to within an error $O(\tau q_\infty / r)$, the flow is equilibrium wedge flow. The shock is straight and the flow is uniform and parallel to the wedge.

It is helpful to keep in mind here the procedure for obtaining the viscous flow over a body: (i) the non-viscous flow is computed ignoring one boundary condition (i.e., tangential velocity equals zero), (ii) the structure of the apparent discontinuity (vortex sheet) at the body is investigated using the boundary layer approximation, (iii) the non-viscous flow over the body plus displacement thickness is computed, etc. For the present problem steps analogous to (i) and (ii) will be taken. Note that here part of the problem is to determine the boundary; that is, the shock wave.

In Figure 7(a) a streamline and the fictitious "equilibrium shock", predicted by the first term of the series expansion, are shown in dashed lines. The transition across the shock is governed by the equilibrium shock relations. The angle of the equilibrium shock is fixed by M_∞ and the wedge angle. Extended, it must go through the tip in order to satisfy the conservation of mass. The actual shock (solid line) must be displaced upstream of the equilibrium shock, but its curvature must vanish to within an error $O(\tau q_\infty / r)$. To this approximation the non-equilibrium flow behind a straight shock describes the flow near the shock but far from the tip (Figure 7(b)). This flow is obtained from the exact solution of Chapter 5. Thus the "boundary layer", or rapid transition region, is determinable. Compared to the equilibrium region between the shock and the body this transition region is negligibly small. It and the shock merge into the equilibrium shock.

The question remains: how to join the two regions; or rather, how far is the shock displaced from the equilibrium shock? This is answered by again invoking the conservation of mass. A transition region streamline must asymptotically approach the equilibrium streamline that originates at the same point of the free stream flow (see Figure 7(b)). The displacement of the shock from the equilibrium shock is denoted by ℓ. From the condition defining ℓ it is easily shown that

$$\ell = b \tan \beta_e / \left[\tan \beta_e - \tan (\beta_e - \theta_e) \right] \qquad (6.12)$$

where β_e is the equilibrium shock angle, θ_e is the wedge angle, and b is the distance (measured perpendicular to the shock) between the shock and the asymptote to the transition streamline (see Figure 7(b) or 3). There is no convenient expression for b, but it is easily determined graphically when equations (5.11) are plotted. For the conditions of the example of an exact solution given in Chapter 5, viz., $\beta_e = 65^\circ$, $\theta_e = 46.7^\circ$, $M_\infty = 8$, in N_2, (6.12) gives

$$\ell = .177\, \tau q_\infty = .0008 \text{ ft.}$$

whereas $\xi_r = .136\, q_\infty \tau$. In Figure 7(c) the two regions are shown according to this approximation; i.e., to within an error $O(\tau q_\infty / r)$. The equilibrium shock is shown extended to the tip. The next approximation, with an error $O(\tau q_\infty / r)^2$, would show the downstream edge of the transition region to be curved.

This next approximation has not yet been worked out. The following is an outline of how this might be done. By developing gradient functions for equilibrium flow, the curvature of the equilibrium shock wave could be obtained. Then let the actual shock have this same curvature. For this curved shock, a shock oriented coordinate system could be used to attempt to get the next approximation to the transition region.

ACKNOWLEDGMENT

The author wishes to thank Dr. J. Sternberg and Mr. G. D. Kahl for their helpful discussions of this work.

Raymond Sedney
RAYMOND SEDNEY

REFERENCES

1. Bethe, H. A. and Teller, E. Deviations from Thermal Equilibrium in Shock Waves. Aberdeen Proving Ground: Ballistic Research Laboratories Report X-117.

2. Ivey, H. R. and Cline, C. W. Effect of Heat-Capacity Lag on Flow Through Oblique Shock Waves. NACA TN-2196, October 1950.

3. Freeman, N. C. Nonequilibrium Flow of an Ideal Dissociating Gas. J. Fluid Mech., Vol. 4, Part 4, August 1958.

4. Moore, F. K. and Gibson, W. E. Propagation of Weak Disturbances in a Gas Subject to Relaxation Effects. J.A.S. Report No. 59-64 (January 26-29, 1959)(Presented at the 27th Annual Meeting).

5. Sternberg, J. Triple Shock-Wave Intersections. Phys. Fluids, Vol. 2, No. 2, pp 179-206, March-April 1959.

6. Wood, W. W. and Kirkwood, J. G. Hydrodynamics of a Reacting and Relaxing Fluid. J. Applied Physics, Vol. 28, No. 4, pp 395-398, April 1957.

7. Hilsenrath J. et al. Tables of Thermal Properties of Gases. National Bureau of Standards, Circular 564, Washington, D. C., Government Printing Office, November 1955.

8. Blackman, V. Vibrational Relaxation in Oxygen and Nitrogen. J. Fluid Mech., Vol. 1, Part 1, pp 61-85, May 1956.

9. Liepmann, H. W. and Roshko, A. Elements of Gasdynamics. John Wiley and Sons, New York, 1957.

10. Broer, L. J. F. On the Influence of Acoustic Relaxation of Compressible Flow. Applied Scientific Research, Vol. A2, pp 447-468, 1951.

11. Thomas, T. Y. On Curved Shock Waves. J. Math. and Phys., Vol. 26, pp. 62-68, 1947.

12. Gerber, N. and Bartos, J. M. Tables for Determination of Flow Variable Gradients Behind Curved Shock Waves. Aberdeen Proving Ground: Ballistic Research Laboratories Report 1086, January 1960.

13. Ames Research Staff. Equations, Tables, and Charts for Compressible Flow. NACA R-1135, 1953.

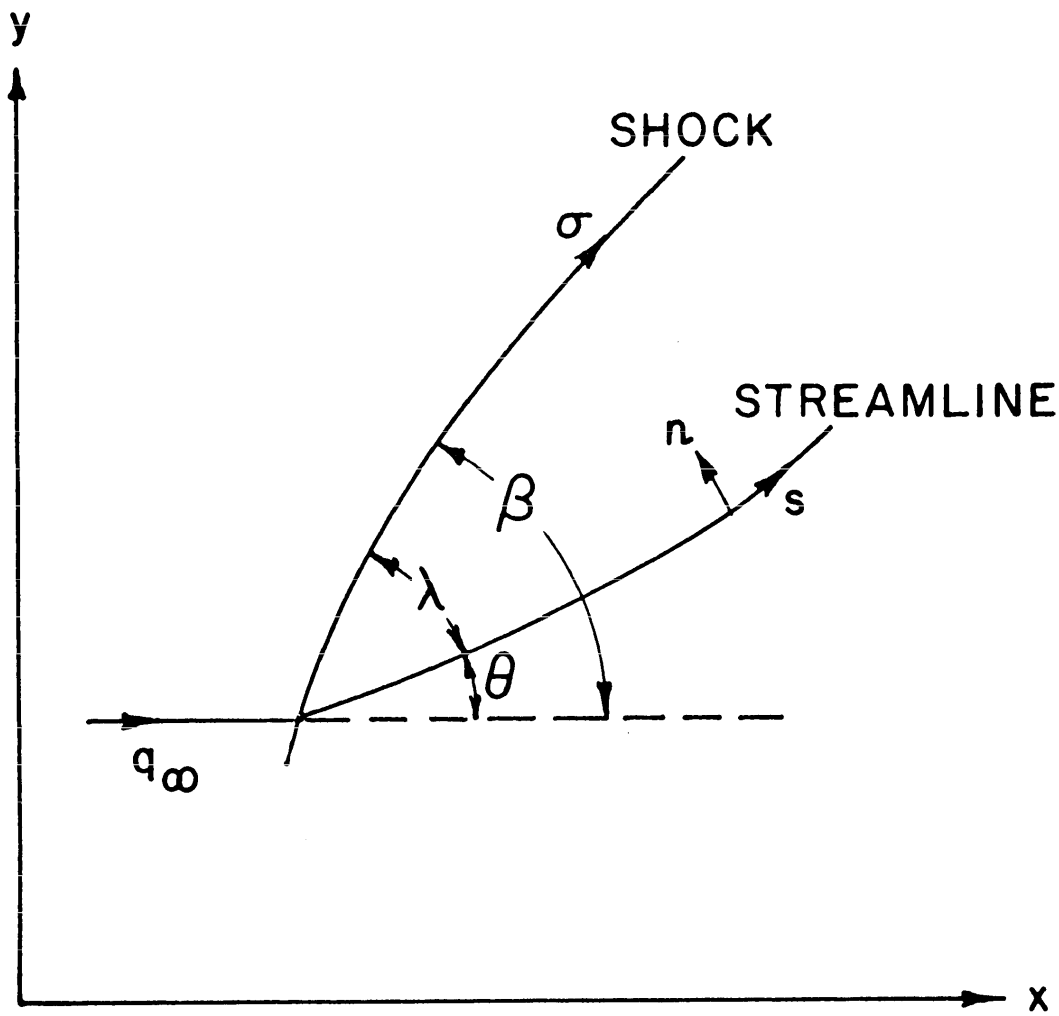

FIGURE 1

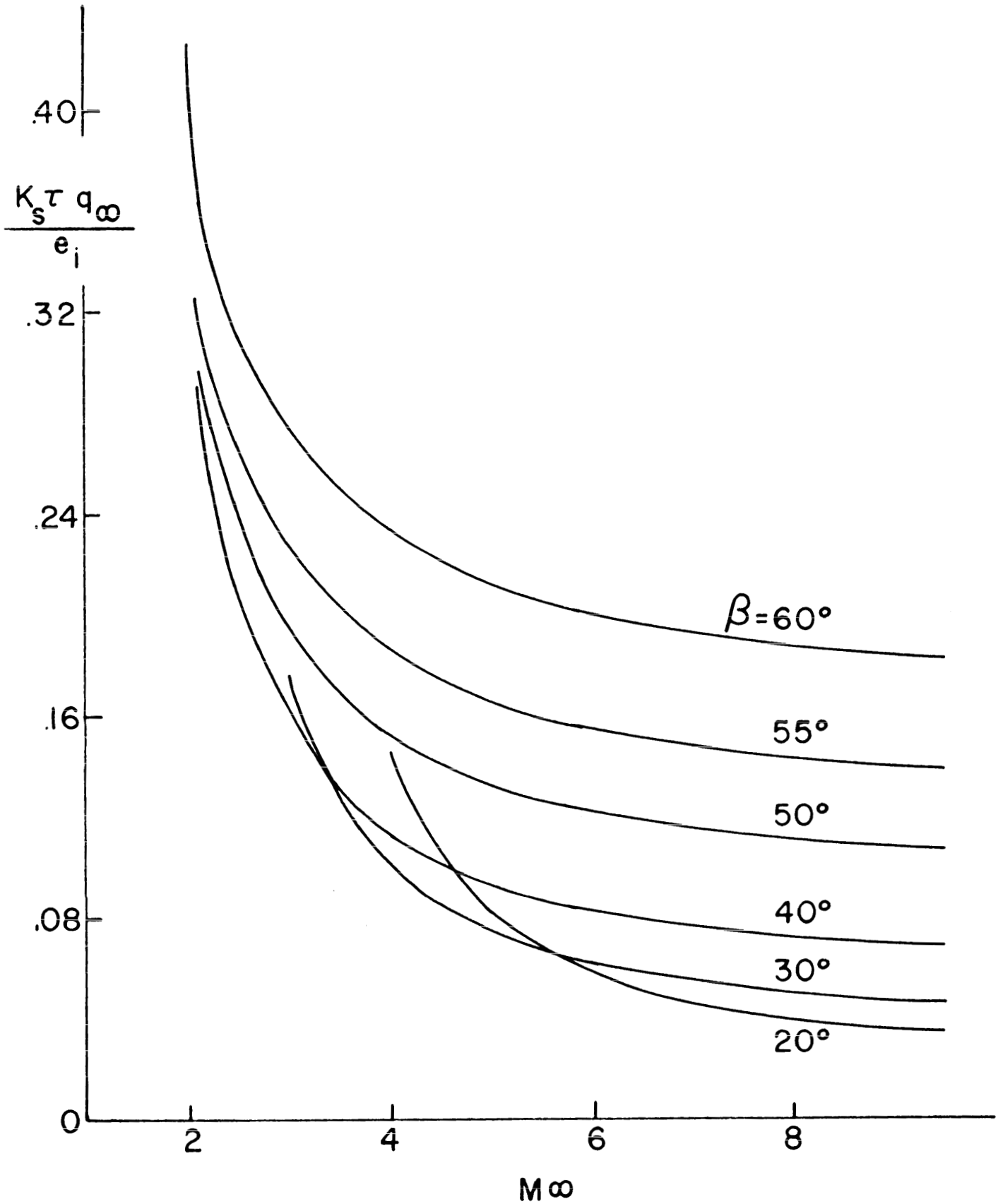
.40
$\frac{K_s \tau q_\infty}{e_i}$
.32
.24
.16
.08
0
2
4
6
8
$M\infty$
β=60°
55°
50°
40°
30°
20°

FIGURE 2

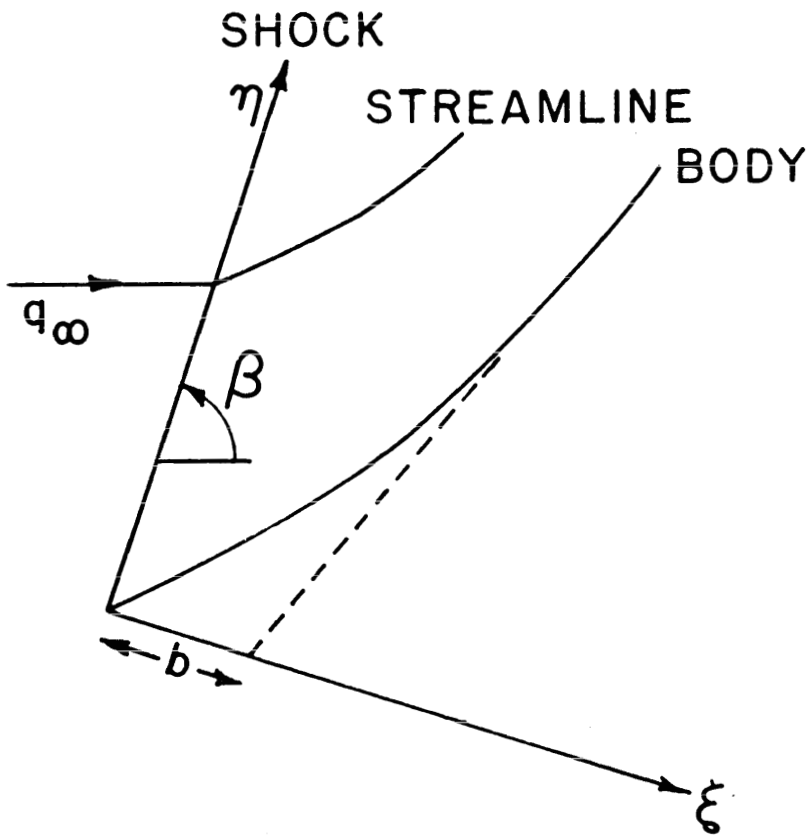

FIGURE 3

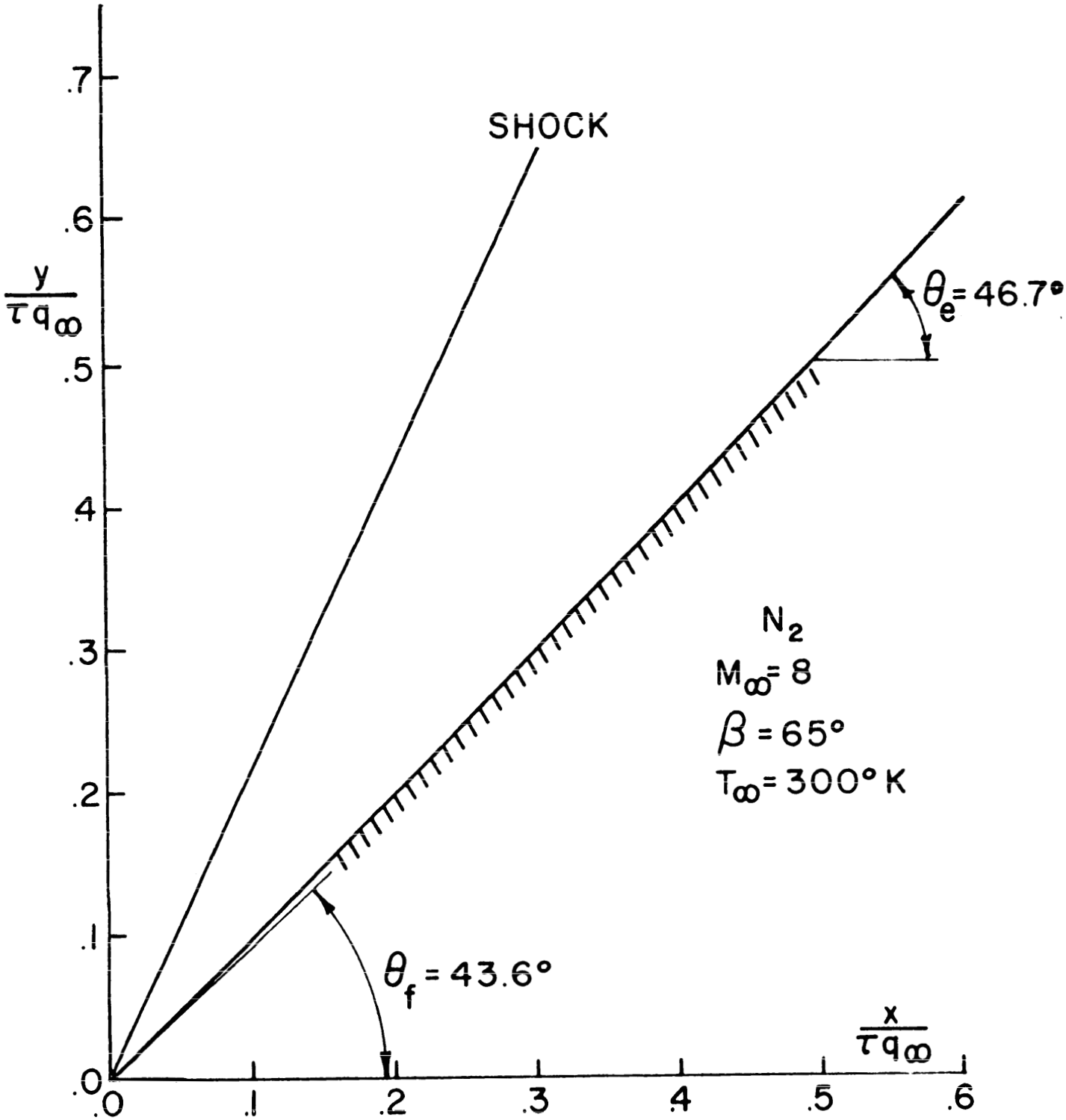
SHOCK
$\frac{y}{\tau q_\infty}$
.7
.6
.5
.4
.3
.2
.1
.0
$\theta_e = 46.7°$
N_2
$M_\infty = 8$
$\beta = 65°$
$T_\infty = 300° K$
$\theta_f = 43.6°$
$\frac{x}{\tau q_\infty}$
.0
.1
.2
.3
.4
.5
.6

FIGURE 4

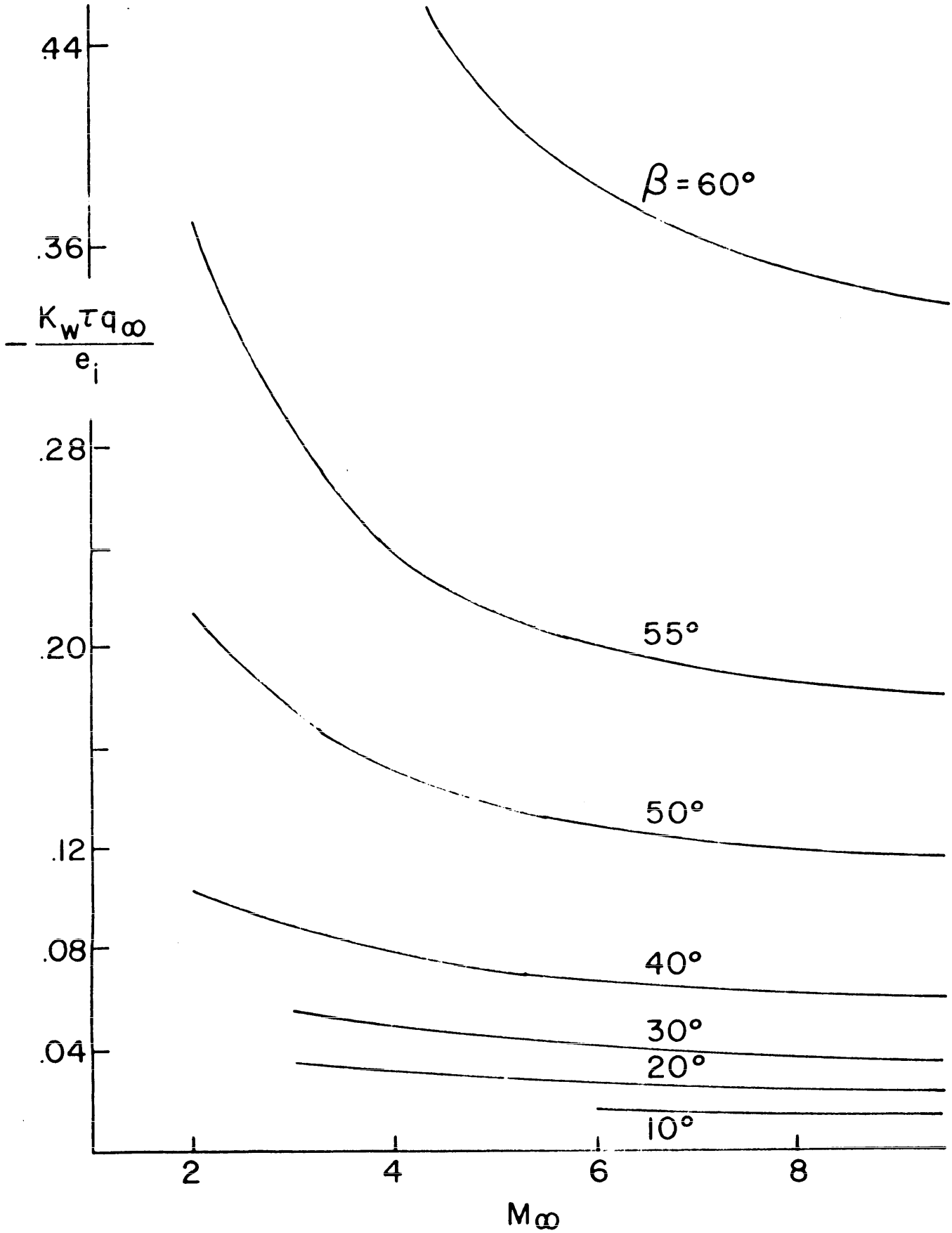
.44
.36
$-\frac{K_w \tau q_\infty}{e_i}$
.28
.20
.12
.08
.04
β = 60°
55°
50°
40°
30°
20°
10°
2
4
6
8
M∞

FIGURE 5

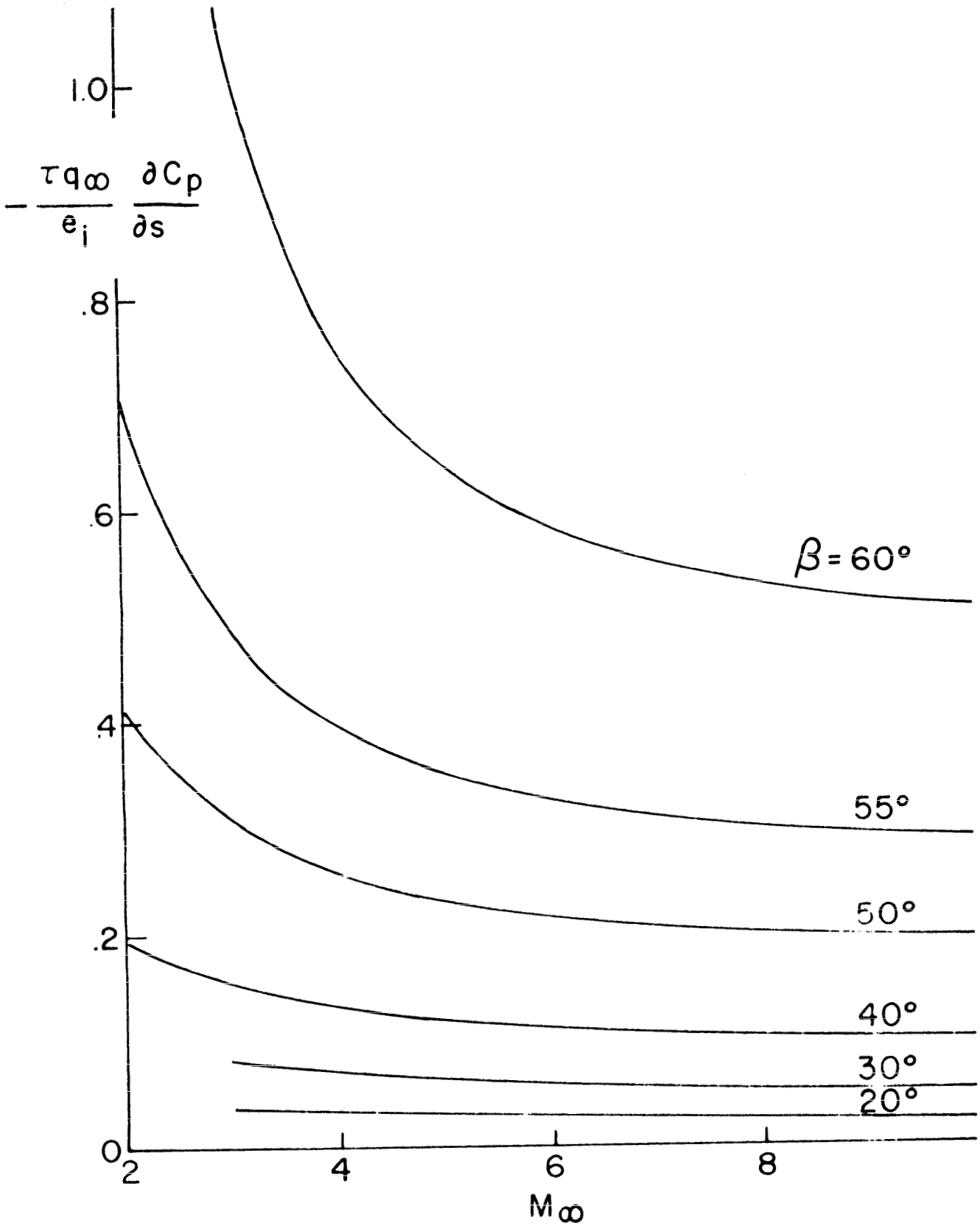
1.0
$-\frac{\tau q_\infty}{e_i}\frac{\partial C_p}{\partial s}$
.8
.6
.4
.2
0
2
4
6
8
M_∞
$\beta = 60°$
55°
50°
40°
30°
20°

FIGURE 6

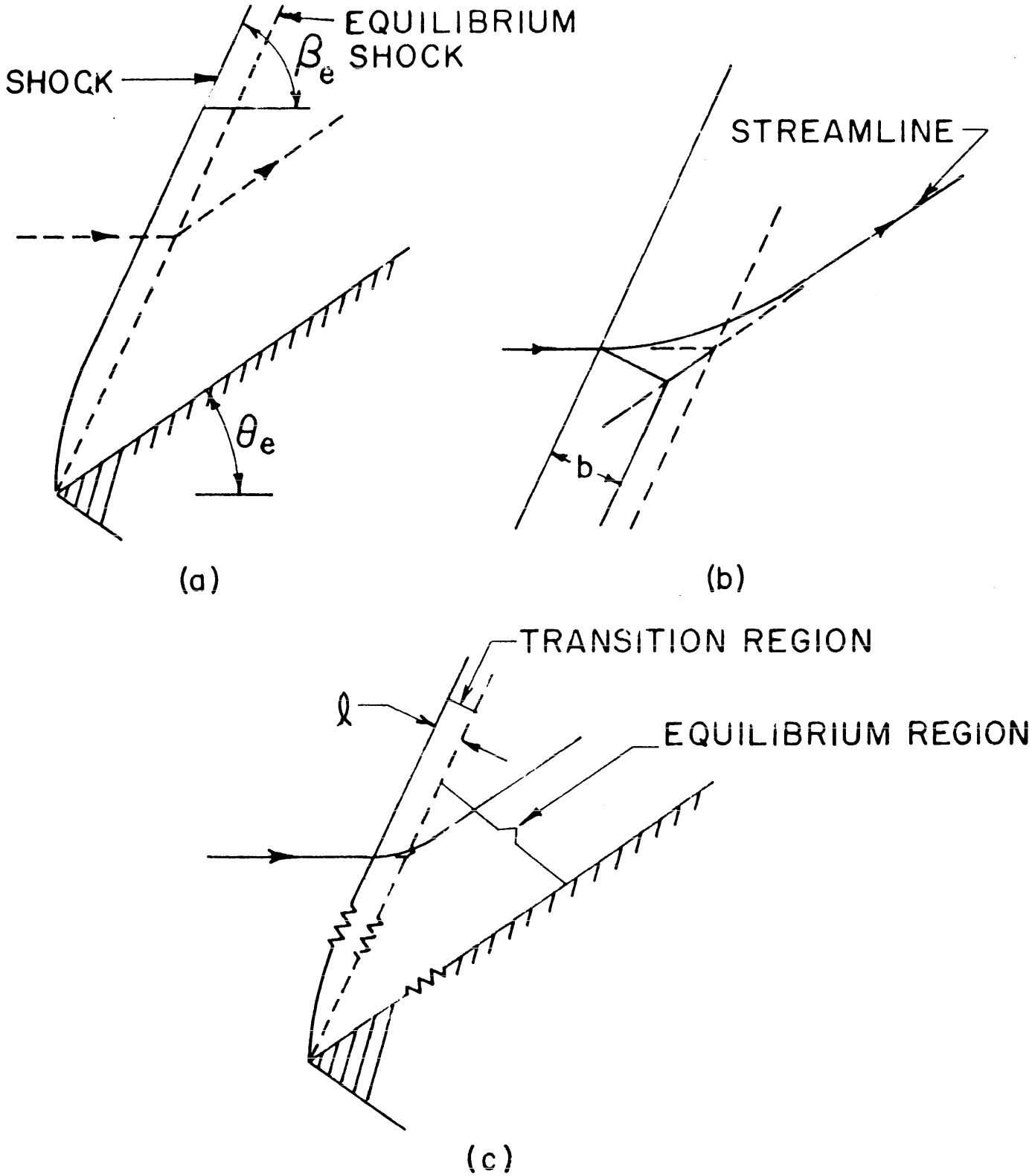
EQUILIBRIUM
SHOCK
SHOCK
β_e
θ_e
(a)
STREAMLINE
b
(b)
TRANSITION REGION
EQUILIBRIUM REGION
ℓ
(c)

FIGURE 7

DISTRIBUTION LIST

No. of Copies	Organization
1	Chief of Ordnance Department of the Army Washington 25, D. C. Attn: ORDTB - Bal Sec
1	Commanding Officer Diamond Ordnance Fuze Laboratories Washington 25, D. C. Attn: ORDTL-012
1	Office of Technical Services Department of Commerce Washington 25, D. C.
10	Director Armed Services Technical Information Agency Arlington Hall Station Arlington 12, Virginia Attn: TIPCR
10	British Joint Services Mission 1800 K Street, N. W. Washington 6, D. C. Attn: Reports Officer
4	Canadian Army Staff 2450 Massachusetts Avenue Washington 8, D. C.
3	Chief, Bureau of Naval Weapons Department of the Navy Washington 25, D. C. Attn: RRRE
2	Commander U. S. Naval Weapons Laboratory Dahlgren, Virginia
2	Commander Naval Ordnance Laboratory White Oak Silver Spring 19, Maryland Attn: Library
1	Commander Naval Ordnance Test Station China Lake, California Attn: Technical Library
1	Superintendent U. S. Naval Postgraduate School Monterey, California
1	Commander Air University Maxwell Air Force Base Alabama Attn: Air University Library (3T-AUL-60-118)
4	Commander Air Research and Development Command Andrews Air Force Base Washington 25, D. C.
1	Director National Aeronautics and Space Administration Lewis Research Center Cleveland Airport Cleveland, Ohio
1	Director National Aeronautics and Space Administration Ames Research Center Moffett Field, California
1	Director National Aeronautics and Space Administration Langley Research Center Langley Field, Virginia Attn: Mr. G. P. Wood

DISTRIBUTION LIST

No. of Copies	Organization
1	Director National Aeronautics and Space Administration 1520 H Street, N. W. Washington 25, D. C. Attn: Division of Research Information
1	U. S. Atomic Energy Commission Los Alamos Scientific Laboratory P. O. Box 1663 Los Alamos, New Mexico
1	Army Research Office Arlington Hall Station Arlington, Virginia Attn: Lt Col J. T. Brown
1	Commanding General Army Ballistic Missile Agency Redstone Arsenal, Alabama Attn: Technical Library
1	Commander Army Rocket & Guided Missile Agency Redstone Arsenal, Alabama Attn: Technical Library ORDXR-OTL
1	Commanding General U. S. Army Ordnance Missile Command Redstone Arsenal, Alabama Attn: Major D. H. Steininger
1	Commanding General White Sands Missile Range New Mexico Attn: ORDBS-TS-TIB
1	Brown University Division of Applied Mathematics Providence 12, Rhode Island Attn: Dr. R. Probstein
2	California Institute of Technology Guggenheim Aeronautical Laboratory Pasadena 4, California Attn: Professor L. Lees Professor H. W. Leipmann
1	Jet Propulsion Laboratory California Institute of Technology 4800 Oak Grove Drive Pasadena 3, California
1	Cornell University Graduate School of Aeronautical Engineering Ithaca, New York Attn: Professor W. R. Sears
1	Duke University Box CM, Duke Station Durham, North Carolina Attn: Dr. R. J. Duffin
2	Princeton University Department of Aeronautical Engineering Princeton, New Jersey Attn: Professor W. Hayes Professor J. Bogdonoff
2	Rensselaer Polytechnic Institute Troy, New York Attn: Professor T. Y. Li Professor G. H. Handelman
1	Stanford University Stanford, California Attn: Dr. M. D. Van Dyke
1	University of Illinois Aeronautical Institute Urbana, Illinois

DISTRIBUTION LIST

No. of Copies	Organization
1	University of Maryland Institute for Fluid Dynamics and Applied Mathematics College Park, Maryland Attn: Mr. S. I. Pai
1	University of Southern California Engineering Center Los Angeles 7, California
1	Arthur D. Little, Inc. 30 Memorial Drive Cambridge 42, Massachusetts
1	Applied Physics Laboratory The Johns Hopkins University 8621 Georgia Avenue Silver Spring, Maryland
1	AVCO Manufacturing Corporation Advance Development Division Research Laboratory 2385 Revere Beach Parkway Everett 49, Massachusetts
1	Boeing Airplane Company Seattle 14, Washington Attn: F. E. Ehlers
1	CONVAIR A Division of General Dynamics Corporation Ordnance Aerophysics Laboratory Daingerfield, Texas
1	CONVAIR A Division of General Dynamics Corporation P. O. Box 1950 San Diego, California Attn: R. D. Linnell
1	Cornell Aeronautical Laboratory, Inc. 4455 Genesee Street Buffalo 5, New York Attn: Dr. F. K. Moore
1	Douglas Aircraft Company 3000 Ocean Park Boulevard Santa Monica, California Attn: Mr. R. J. Hakkinen
1	Firestone Tire and Rubber Company Defense Research Division 1200 Firestone Parkway Akron 17, Ohio
2	General Electric Company Aeronautics and Ordnance Systems Division 1 River Road Schenectady 5, New York Attn: Dr. H. T. Nagamatsu Dr. D. R. White
1	General Electric Company Missile and Space Vehicle Department 3198 Chestnut Street Philadelphia, Pennsylvania Attn: Dr. F. G. Gravalos
1	North American Aviation, Inc. 12214 Lakewood Boulevard Downey, California Attn: Aerophysics Laboratory
1	Lockheed Missiles and Space Division 3251 Hanover Street Palo Alto, California Attn: Dr. D. Bershader

DISTRIBUTION LIST

No. of Copies	Organization
1	Glenn L. Martin Company Baltimore 3, Maryland Attn: S. C. Traugott
1	Space Technology Laboratories, Inc. P. O. Box 95001 Los Angeles 45, California
1	Ramo-Wooldridge Corporation 5730 Arbor Vitae Street Los Angeles 45, California
1	Professor G. F. Carrier Division of Engineering and Applied Physics Harvard University Cambridge 38, Massachusetts
1	Professor F. H. Clauser, Jr. The Johns Hopkins University Department of Aeronautics Baltimore 18, Maryland
1	Professor H. W. Emmons Harvard University Cambridge 38, Massachusetts
1	Dr. A. E. Puckett Hughes Aircraft Company Systems Development Laboratories Florence Avenue at Teal Street Culver City, California
1	Dr. L. H. Thomas Watson Scientific Computing Laboratory 612 West 116th Street New York 25, New York